Nucleation and polymorph selection in a model colloidal fluid

Andrea Robben Browning,[1] Michael F. Doherty,[1] and Glenn H. Fredrickson[1,2,3]
[1]*Department of Chemical Engineering, University of California, Santa Barbara, California 93106, USA*
[2]*Department of Materials, University of California, Santa Barbara, California 93106, USA*
[3]*Materials Research Laboratory, University of California, Santa Barbara, California 93106, USA*
(Received 14 January 2008; published 15 April 2008)

Understanding and controlling polymorph selection is important because the structure of a crystal is critical to its properties. We have explored polymorph selection during nucleation in the hard-core repulsive Yukawa fluid. This model has two polymorphs (bcc and fcc), the relative stability of which can be adjusted by changing the potential parameters. We used seeded molecular-dynamics simulations to follow the evolution of the metastable bcc structure in the fcc stable region. It was found that the degree of undercooling affected the development of the bcc seeds. At small undercoolings, the bcc seed became a bcc crystal, but at large undercoolings bcc seeds became fcc crystals. Homogenously nucleated simulations were also compared to colloidal experiments. The simulations yielded nuclei of similar shape to the experimentally observed nuclei and a similar minimum size of growth. The simulated nuclei had more bcc signature than the experimental nuclei, but upon further growth the bcc signature faded, indicating that the difference between simulations and experiments may be due to the experimental nuclei having more time to resolve their structure.

DOI: 10.1103/PhysRevE.77.041604 PACS number(s): 64.60.qe, 82.70.Dd

I. INTRODUCTION

Solid nucleation has become a growing topic of study in recent years because of its importance in crystal structure development, crystallization time, and crystal size. It has long been a topic of scientific interest, but until the recent advances in both simulation (e.g., more efficient algorithms and increased computing power) and experiments (e.g., development of model colloidal and protein systems) nucleation has proved difficult to study. With the present technology, the governing principles of nucleation and growth phenomena are beginning to unfold.

One area where nucleation is of particular importance is polymorph development. Understanding polymorphs, different crystal structures of the same molecule, is crucial to the final utility of any crystalline product. Properties such as stability, hardness, and bioavailability can be different among polymorphs [1]. Given the effect on crystal properties it is important to establish a method for predicting polymorph formation in both laboratory and industrial crystallization. Lack of knowledge of which phenomena and physical properties determine polymorph formation has prevented useful predictive tools from being developed.

As the first stage of crystal development, it is natural to explore nucleation for controlling factors of polymorph selection. This is supported by recent experiments that indicate that nucleation is important in fixing crystal structure [2]. Experiments have also suggested that seeding with the desired polymorph is not sufficient to ensure growth of the desire polymorph [3]. These and other experimental findings support the study of nucleation to discover the factors controlling polymorph formation.

However, nucleation is difficult to study experimentally. The low concentration and small size of nuclei make it difficult to distinguish them from the parent solution. It is also challenging to ensure that the nuclei are observed in early stages, before significant growth has occurred. Despite these difficulties, nucleation has been directly observed in large-particle experiments [2,4]. Large particles such as colloids form nuclei large enough to be observed by techniques such as optical microscopy and nucleate slowly enough to be investigated before significant growth has occurred. Critical nuclei of 25–100 particles with nonspherical cluster shape and structure of the stable polymorph were observed in both protein and colloidal nucleation experiments. From measurements on these systems, new insights into nucleation have been gained.

The advances in experimental procedures that allowed for studies of large-particle nucleation have been matched by advances in simulation techniques. Increases in computing speed and the development of advanced computational techniques have yielded new insights into the fundamentals of nucleation. The majority of simulations have been limited to model fluids with simple pair-additive potentials [5–9], but a few studies of realistic molecules have been performed. The model particle simulations behave similar to the protein and colloid experiments. They find critical nuclei of approximately 100 particles, but they observe some percentage of the metastable polymorph. More realistic molecular simulations of Si and N_2 [10,11] have critical nuclei of near-spherical shape with approximately 50 (1.2 nm in diameter) and 300 molecules, respectively.

The current work examines polymorph selection in the hard-core repulsive Yukawa fluid using molecular-dynamics simulations. The hard-core repulsive Yukawa potential has two reported polymorphs (bcc and fcc) [12] of varying stability allowing for the study of the effect of nucleation on polymorph selection. The model system and the simulation methods are described in Sec. II. In Sec. III, seeding of small crystallites is used to explore the parameter space of the hard-core repulsive Yukawa fluid. We have found that the reported fcc region of stability actually contains a subregion in which mixed fcc and hcp structures occur. However, we have only used bcc or fcc seeds, since there is no evidence that a pure hcp stable phase exists. By using molecular dy-

namics along with a potential with multiple polymorphs, the role of structure in the early stages of crystal growth can be further examined. In Sec. IV, homogenous nucleation of the hard-core repulsive Yukawa fluid is compared to colloidal experiments [4]. This ability to compare the simulations to experiments allows for the validation of the simulation methods along with confirmation of early nuclei attributes.

II. NUCLEATION MODEL SYSTEM AND SIMULATION METHODS

The current study uses molecular-dynamics simulations of model particles to further explore nucleation with a particular focus on polymorph selection. The model potential is the hard-core repulsive Yukawa (also known as screened Coulomb) potential [12]. This potential was chosen because of the occurrence of three phases (bcc, fcc, and fluid), the stability of which can be adjusted with the model parameters, and the connection with colloid nucleation experiments [4]. The potential is a pair interaction potential and is described by

$$U = \begin{cases} \infty, & r < \sigma, \\ \epsilon \dfrac{\exp[-\kappa\sigma(r/\sigma - 1)]}{r/\sigma}, & r \geq \sigma, \end{cases} \tag{1}$$

where U is the interaction energy between two particles, r is the center-of-mass distance between particles, σ is the hard-core diameter, ϵ is the energy parameter, and $1/\kappa$ is the screening length. The potential can be nondimensionalized by ϵ and σ to give the nondimensional quantities [12] $\tilde{U} = U/\epsilon$, $\tilde{r} = r/\sigma$, $\tilde{\kappa} = \kappa\sigma$, and $\tilde{T} = k_b T/\epsilon$.

The stability of bcc, fcc, and fluid phases can be adjusted using three parameters: reduced temperature ($\tilde{T}$), reduced screening length ($1/\tilde{\kappa}$), and packing fraction ($\eta = N\pi\sigma^3/6V$). At small screening length (near the hard-sphere limit $\tilde{\kappa} \to \infty$) fcc is the stable solid structure. As the fluid approaches the Coulomb limit ($\tilde{\kappa} \to 0$), bcc becomes the stable solid structure. The size of the bcc region of stability relative to the fcc region of stability increases with decreasing $\tilde{T}$. The solid-fluid coexistence line is also affected by temperature; it moves to lower packing fractions as $\tilde{T}$ decreases.

The parameter space was explored using molecular-dynamics simulations. The use of molecular-dynamics simulations allows for the evolution of the nuclei to be observed and structural changes to be monitored kinetically. The simulations were carried out with constant N-V-T [13] using the Nose-Hoover thermostat with reversible integrators developed by Martyna *et al.* [14]. The simulation box was cubic with periodic boundary conditions [13]. The hard core was treated as described by McNeil and Madden [15]. The time step was 0.005 in dimensionless time units [$\tilde{t} = t/(\sigma\sqrt{m/\epsilon})$, where m is the mass of one particle], and the simulation box contained 32 000 particles.

During the simulation, particles in a solid environment were identified using the Steinhardt bond-order parameter method [16,17]. Using the spherical harmonics $Y_{lm}(\theta_{ij}, \phi_{ij}) = Y_{lm}(\hat{\mathbf{r}}_{ij})$ where $\hat{\mathbf{r}}_{ij}$ gives the orientation of the center-to-center vector between particles i and j, the local structure around particle i can be found by

$$\bar{q}_{lm}(i) \equiv \frac{1}{N_b(i)} \sum_{j=1}^{N_b(i)} Y_{lm}(\hat{\mathbf{r}}_{ij}), \tag{2}$$

where $N_b(i)$ is the number of neighbors of particle i. The $l = 6$ harmonics can be used to differentiate between solid and liquid by examining the dot product $\mathbf{q}_6(i) \cdot \mathbf{q}_6(j)$ (hereafter denoted as $q_6 q_6$). The components $q_{6m}(i)$ of the complex vector $\mathbf{q}_6(i)$ are given by

$$q_{6m}(i) \equiv \frac{\bar{q}_{6m}(i)}{[\sum_{m=-6}^{6} |\bar{q}_{6m}(i)|^2]^{1/2}}. \tag{3}$$

A particle-particle association was considered solidlike if $q_6 q_6 > 0.5$ and a particle was considered in a solid environment if it was involved in more than seven solidlike associations.

The difficulty of using molecular dynamics to study rare events such as nucleation was circumvented by using a seeding technique. At some conditions homogeneous nucleation was observed as discussed in Sec. IV. A seed of predetermined structure, shape, and size was constructed and then added to an equilibrated liquid. Any overlaps such that $r < 0.5\sigma$ created by inserting the seed were removed using the algorithm described by Jodrey and Tory [18] before beginning the simulations. Remaining overlaps were removed in the initial steps of the simulations. Perfect structure seeds were primarily used, but a test simulation with a seed created by removing a section of a fully equilibrated crystal yielded the same results as a perfect seed. Only spherical seeds are reported in this study, but other shapes were also simulated. Nonsmooth shapes (i.e., cubes) were observed to become spherelike early in the simulation. During the molecular-dynamics (MD) simulations, the seeds were monitored visually for changes in shape. The final structure of the fully crystalline system was also compared to the initial structure of the seed. The final structure was determined by comparing the pair distribution function of the final structure to reference pair distribution functions [19] for bcc and fcc. The reference pair distribution functions were obtained by equilibrating a full simulation box of the desired structure in a region of known stability of that structure.

III. RESULTS AND DISCUSSION

Simulations were performed at three different values of $1/\tilde{\kappa}$: 0.05, 0.1, and 0.2. At these values of $1/\tilde{\kappa}$, $\tilde{T}$-v-η parameter space was explored by conducting seeded simulations in the solid region. The parameter space is defined by fluid-fcc melting data points taken from Hynninen and Dijkstra [12], but the melting behavior was verified with simulations. The only stable structure is fcc for values of $1/\tilde{\kappa}$ of 0.1 and 0.05, but at $1/\tilde{\kappa} = 0.2$ both a bcc and a fcc region of stability occur. In the fcc region of stability, seeds of the metastable bcc structure were simulated. fcc seeds are not reported in this region, since they grew as expected into a

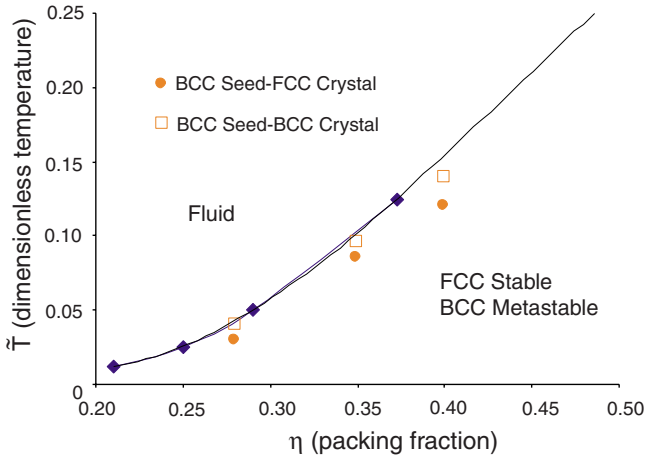

FIG. 1. (Color online) Polymorphic behavior of the hard-core repulsive Yukawa fluid for $1/\tilde{\kappa}=0.1$. The solid (blue) diamonds are the fluid-fcc melting data points taken from Hynninen and Dijkstra [12]. These points are connected and extrapolated. The simulation points are differentiated by the seed structure and final crystal structure: bcc-seed–bcc-crystal structure: open (orange) squares. bcc-seed–fcc-crystal structure: solid (orange) circles.

stable fcc solid. In the bcc region of stability both fcc (to determine the metastable structure behavior) and bcc seeds (to determine minimum size of seed needed for growth in this narrow region of the parameter space where only small undercoolings are possible) were simulated.

As is well known, the size of a critical nucleus depends sensitively on the degree of undercooling. Simulations close to the melting curve are expected to yield critical nuclei substantially larger than at higher undercooling. No attempt to determine the critical size nucleus was made in this portion of the study, but in Sec. IV a critical size is discussed. Seeds of ~2000 particles were attempted first. If they did not grow, the seed size was increased until the seed grew. Seeds between ~8400 particles and ~2000 particles were used in the fcc region of stability. In the bcc region of stability for $1/\tilde{\kappa}=0.2$, much larger seeds were needed (~16 000 particles).

The structure development of bcc seeds for $1/\tilde{\kappa}=0.1$ is shown in Fig. 1. Simulation conditions where bcc seeds were observed to grow into fcc crystals are denoted by solid circles, and where bcc seeds grew into bcc crystals, open squares are used. The fluid-fcc melting data points taken from Hynninen and Dijkstra [12] are shown with solid diamonds. These points are connected and extrapolated to give the melting line. The melting line is divided into two portions: known and extrapolated. Where the melting behavior is known (values of $\tilde{T}\leq 0.125$ and values of $\eta\leq 0.37$), the structure development of the bcc seeds is different depending on the degree of undercooling (distance from the melting curve). At small undercoolings (<9.4%), bcc seeds were observed to grow into bcc crystals that remained stable in extended MD simulations. At large undercoolings (>22%), bcc seeds were observed to become fcc crystals. In the region below the extrapolated portion of the melting curve, the development of fcc crystals from bcc seeds is also observed with results that are similar to the region below the known portion of the melting curve.

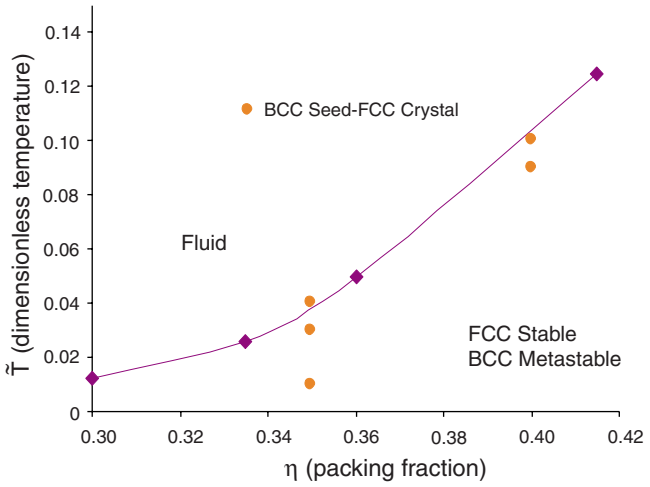

FIG. 2. (Color online) Polymorphic behavior of the hard-core repulsive Yukawa fluid for $1/\tilde{\kappa}=0.05$. Same symbol descriptions as for Fig. 1.

The qualitative effect of undercooling observed for $1/\tilde{\kappa}=0.1$ is also seen for $1/\tilde{\kappa}=0.05$, as shown in Fig. 2. In Sec. IV, the behavior for $1/\tilde{\kappa}=0.05$ will be described in detail and compared to experiments. Homogenous nuclei appear at the higher undercoolings, but the seeds grow to fill the simulation box and incorporate the homogenous nuclei. At this screening length, bcc seeds were always observed to become fcc crystals even at very small undercoolings, indicating that in addition to undercooling, the strength of interparticle interactions affects the effectiveness of the seeding.

At $1/\tilde{\kappa}=0.2$ (see Fig. 3), the existence of a bcc region of stability enables the study of the effect of undercooling on fcc seeds. The symbols defined for Fig. 1 are used for Fig. 3, but three phase transition curves are present at $1/\tilde{\kappa}=0.2$. The

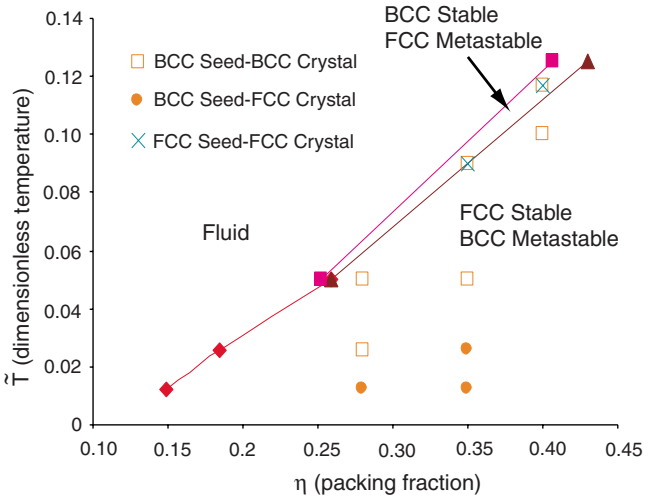

FIG. 3. (Color online) Polymorphic behavior of the hard-core repulsive Yukawa fluid for $1/\tilde{\kappa}=0.2$. The solid (pink) squares are the fluid-bcc melting data points, the solid (brown) triangles are bcc-fcc data points, and the solid (red) diamonds are the fluid-fcc melting data points taken from Hynninen and Dijkstra [12]. Simulation conditions where fcc seeds grew into fcc crystals are denoted by an (light green) X. Other symbols are defined in Fig. 1.

fluid-fcc melting curve is denoted with a solid line and solid diamonds as in Figs. 1 and 2. The fluid-bcc melting curve is denoted by solid squares, and the bcc-fcc equilibrium curve is shown with solid triangles. In the fcc region of stability below the bcc region of stability ($\eta > 0.26$), bcc seeds behave similar to that observed for $1/\tilde{\kappa}=0.05$ and 0.1; however, bcc seeds growing into bcc crystals was observed at much larger undercoolings. This may indicate that the presence of a bcc stable region, stabilizes the bcc structure even in the fcc stable region.

In the bcc region of stability fcc seeds were observed to grow into fcc crystals. Given the small size of the bcc stable region, it is not possible to achieve large undercoolings. Therefore, lack of observing a fcc seed grow into a bcc crystal does not exclude the possibility of such an event. In this region, bcc seeds grew into bcc crystals as expected.

The spherically shaped seeds were observed to become slightly elongated with a roughened surface early in the evolution process. The elongation was observed visually and confirmed by fitting the seed with a ellipsoid. Early in the evolution process the best fitting ellipsoid was found to have a major to minor axis ratio of 1.2 or greater. This observation, along with results discussed in Sec. IV suggests that the stable shape of small crystallites is elliptical.

IV. COMPARISON TO COLLOIDAL EXPERIMENTS

Colloidal systems provide many advantages over small molecules and atoms for the study of nucleation. With slower time scales and larger size, colloidal nucleation is easier to observe experimentally. Similarly, the ability to approximate colloidal systems by simple potentials makes direct comparison of theory and experiment possible. The availability of both experiments and simulations make colloidal systems ideal for fundamental studies of nucleation and validation of nucleation simulations.

Gasser *et al.* [4] have used a colloidal system to measure the critical nucleus size and shape. The colloids were made of poly(methyl methacrylate) sterically stabilized with poly-12-hydroxystearic acid and dyed with rhodamine. The solvent was a mixture of decahydronaphthalene and cyclohexane which closely matches the colloid's refractive index and density. Nucleation was observed by using fast-laser-scanning confocal microscopy. The colloids have an interaction potential in the solvent close to that of hard spheres, so the system can be well approximated by the hard-core repulsive Yukawa fluid with a small value of the screening length. In the application of the hard-core repulsive Yukawa fluid to the colloidal system of Gasser *et al.* the solvent is treated implicitly with all solvent effects assumed to be contained in the interaction potential. Using the hard-core repulsive Yukawa fluid, homogenous nucleation simulations were performed and compared to the experiments.

The simulations were performed with $1/\tilde{\kappa}=0.05$ and $\tilde{T}=0.125$. At these conditions the freezing and melting packing fractions of the hard-core repulsive Yukawa fluid described in the literature [12] (0.39 and 0.41, respectively) are near the packing fractions quoted in the colloidal experiments (0.38 and 0.42, respectively). In Fig. 4 the experimental

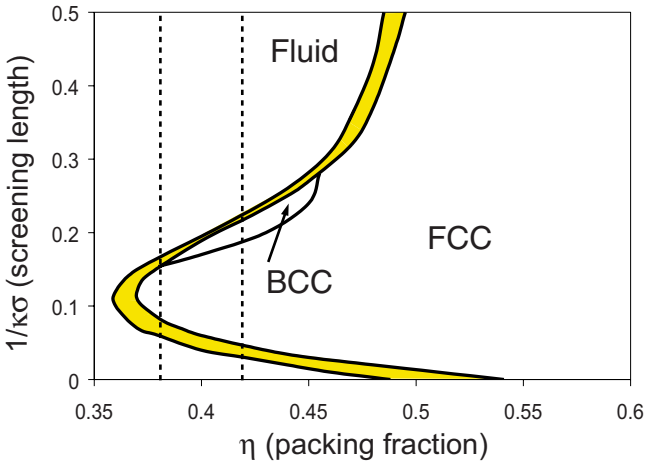

FIG. 4. (Color online) Hard-core repulsive Yukawa behavior at $\tilde{T}=0.125$. Redrawn from Hynninen and Dijkstra [12]. The shaded (yellow) area is the fluid-solid coexistence region. The freezing and melting packing fractions for the experimental system are shown with dotted lines.

freezing and melting packing fractions are shown with dotted lines. It can be observed that $1/\tilde{\kappa}=0.05$ is not the only screening length where the model and experimental freezing and melting packing fractions agree, but it is the only condition where both freezing and melting packing fractions match. The model and experimental freezing and melting packing fractions differ slightly at $1/\tilde{\kappa}=0.05$, but the conditions of the experiments and simulations are well inside the fcc region of stability, ensuring that large undercoolings exist in both the simulations and experiments. fcc is the only stable structure at these conditions. Three different packing fractions within the solid region were simulated: $\eta=0.45$, 0.47, and 0.50. Four similar packing fractions were evaluated in the experiments: $\eta=0.43$, 0.45, 0.47, and 0.49. The use of several packing factions in the same area demonstrate the reproducibility of the results. No seeding was necessary since homogenous nucleation was observed early in the simulations. The location of the spinodal stability limit of the metastable liquid phase in the crystal region of the fluid is not known. If crystallization occurs in the spinodal region, it proceeds spontaneously, not by a nucleation mechanism [9,20]. Though nucleation occurred quickly, it is believed that spinodal decomposition is not occurring since small crystallites were observed to melt.

In addition to using the Steinhardt bond-order parameter method for solid-particle identification, an extended parameter method using histograms of the q_6, q_4, and w_6 parameters was used to determine the structure of the solid particles [16,21,22]. Solid particles were also grouped into clusters by considering two solid particles to be in the same cluster if they are near neighbors by the same definition used in the solid determination step [22].

Several nuclei were observed in the simulations. Similar nuclei shapes were observed when the solid environment criteria was relaxed to five solidlike associations. All nuclei were elongated in shape with a rough surface or ramified with several tendrils. The elongated shape was confirmed by fitting the nuclei with an ellipsoid. The major to minor axis

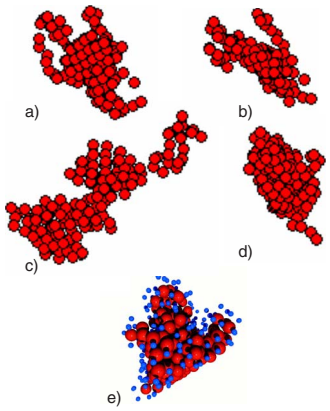

FIG. 5. (Color online) Homogenously nucleated clusters grown at η=0.47 (a), (b), (c) and η=0.45 (d). Particles are shown smaller than actual size for clarity. Parts (a) and (b) are the same cluster shown from two angles. An experimental nucleus is shown in (e) for comparison. From Gasser *et al.* [4]. Reprinted with permission from AAAS.

ratio was found to be 3.5 or greater. This elongated shape is different than the faceted Wulff equilibrium shape [23,24] which would be expected in the classical nucleation theory [25]. In some systems, however, faceted nuclei have been observed in simulations—e.g., NaCl [26].

One nucleus is shown in Figs. 5(a) and 5(b) from two angles to illustrate the elongated shape of the nuclei. Two other nuclei are also shown in Figs. 5(c) and 5(d). The nuclei shown in (a)–(c) were grown at η=0.47. The nucleus in (d) was grown at η=0.45. It can be observed that though all the nuclei shown are different, they have similar characteristics. Figure 5(e) shows an experimental nucleus for comparison, and the qualitative similarity with the simulated nuclei can be seen.

The simulated nuclei contained a mixture of bcc, fcc, hcp, and fluid. The *initial* structure (after approximately 0.03 s of real time, with the nondimensional time converted to real time using the parameter of Gasser *et al.* of σ=2.52 μm and assuming room temperature, 25 °C and colloid density of 1.196 g/cm^3) of the nuclei found in simulations contained 7%–27% bcc, 14%–46% fcc, 0%–16% hcp, and 29%–77% fluid. Upon further crystal growth the amount of bcc signature diminished to 0%–3%. The structure of the experimental nuclei, which were observed after at least 20 min, contained 0%–3% bcc, 10%–58% fcc, 20%–32% hcp, and 22%–58% fluid. The bond-order parameter histograms of the initial simulation nuclei were wider than those for the experimental nuclei, and the histogram fit was worse. In the experiments, nucleation occurred more slowly than in the simulations (expected since hydrodynamic forces and interactions are ignored in the simulations) and the additional time may have allowed for more structure resolution before growth. The observation of a significant bcc signature in early nuclei was also observed in other simulations of Lennard-Jones, Yukawa, and hard-core Yukawa particles [17,27,28].

To determine the minimum size of growth for an fcc crystallite, seeded simulations were used. A minimum size of growth of approximately 150 particles (between 62 and 266 particles). Though the undercooling was different for different values of η, the minimum size of growth remained in the same range. The minimum size of growth found in the simulations agrees well with the critical nucleus size of approximately 100 particles found in the experiments.

V. CONCLUSIONS

We have shown that polymorph development in the hard-core repulsive Yukawa fluid is directed by the degree of undercooling and strength of the interparticle interaction. This was demonstrated using seeded molecular-dynamics simulations, where seeds of a metastable polymorph were observed to persist only for small undercoolings and transformation to the stable crystal form occurred at large undercooling. The degree of undercooling necessary for transformation to the stable structure depends on the strength of interparticle interactions, with very weak interactions always yielding the stable structure. A comparison of simulation results to colloidal experiments was also made. The similarity in shape characteristics and minimum size of growth support the applicability of simulations to understand and reproduce experimental nucleation studies. We believe that the appearance of more bcc signature in the initial stages of simulation relative to the experiments is caused by the difference in time scales between the two methods, which allow for the experimental nuclei to experience more structural refinement. In future work, the techniques utilized here will be applied to simulations of realistic small molecules with explicit solvent.

ACKNOWLEDGMENTS

The work of A.R.B. was supported by the National Science Foundation and the UC Regents. M.F.D. and G.H.F. acknowledge partial funding from the National Science Foundation under Grants Nos. CBET-0651711 and DMR-0603710, respectively. This work made use of the UCSB MRL Central Facilities supported by the MRSEC Program of the National Science Foundation under Grant No. DMR05-20415.

[1] J. Bernstein, *Polymorphism in Molecular Crystals* (Oxford Science, Oxford, 2002).
[2] S. Yau and P. Vekilov, J. Am. Chem. Soc. **123**, 1080 (2001).
[3] L. Yu, J. Am. Chem. Soc. **125**, 6380 (2003).
[4] U. Gasser, E. Weeks, A. Schofield, P. Pusey, and D. Weitz, Science **292**, 258 (2001).
[5] E. Meijer and D. Frenkel, J. Chem. Phys. **94**, 2269 (1991).
[6] B. O'Malley and I. Snook, Phys. Rev. Lett. **90**, 085702 (2003).
[7] J. Anwar and P. Boateng, J. Am. Chem. Soc. **120**, 9600 (1998).

[8] S. Auer and D. Frenkel, J. Chem. Phys. **120**, 3015 (2004).
[9] F. Trudu, D. Donadio, and M. Parrinello, Phys. Rev. Lett. **97**, 105701 (2006).
[10] S. Izumi, S. Hara, T. Kumagai, and S. Sakai, J. Cryst. Growth **274**, 47 (2005).
[11] J. M. Leyssale, J. Delhommelle, and C. Millot, Chem. Phys. Lett. **375**, 612 (2003).
[12] A.-P. Hynninen and M. Dijkstra, Phys. Rev. E **68**, 021407 (2003).
[13] D. Frenkel and B. Smit, *Understanding Molecular Simulation* (Academic, San Diego, 2002), 2nd edition.
[14] G. J. Martyna, M. E. Tuckerman, D. J. Tobias, and M. L. Klein, Mol. Phys. **87**, 1117 (1996).
[15] W. J. McNeil and W. G. Madden, J. Chem. Phys. **76**, 6221 (1982).
[16] P. J. Steinhardt, D. R. Nelson, and M. Ronchetti, Phys. Rev. B **28**, 784 (1983).
[17] P. R. ten Wolde and D. Frenkel, Phys. Chem. Chem. Phys. **1**, 2191 (1999).
[18] W. S. Jodrey and E. M. Tory, Phys. Rev. A **32**, 2347 (1985).
[19] M. Allen and D. Tildesley, *Computer Simulation of Liquids* (Oxford Science, Oxford, 1987).
[20] M. G. Noro, N. Kern, and D. Frenkel, Europhys. Lett. **48**, 332 (1999).
[21] Y. Wang and C. Dellago, J. Phys. Chem. B **107**, 9214 (2003).
[22] P. R. ten Wolde, M. Ruiz-Montero, and D. Frenkel, J. Chem. Phys. **104**, 9932 (1996).
[23] C. Jayaprakash and W. F. Saam, Phys. Rev. B **30**, 3916 (1984).
[24] G. Wulff, Z. Krystallogr. **34**, 449 (1901).
[25] I. V. Markov, *Crystal Growth for Beginners*, 2nd ed. (World Scientific, Singapore, 2003).
[26] C. Valeriani, E. Sanz, and D. Frenkel, J. Chem. Phys. **122**, 194501 (2005).
[27] C. Desgranges and J. Delhommelle, J. Chem. Phys. **126**, 054501 (2007).
[28] S. Auer and D. Frenkel, Annu. Rev. Phys. Chem. **55**, 333 (2004).